JOURNAL OF SOLID STATE CHEMISTRY 46, 162–171 (1983)

Heat Capacity of Vanadium–Oxygen Alloy

HIDEAKI INABA, SEIICHI TSUJIMURA, AND KEIJI NAITO

Department of Nuclear Engineering, Faculty of Engineering, Nagoya University, Furo-cho, Chikusa-ku, Nagoya, Japan

Received June 8, 1982; in revised form August 9, 1982

Heat capacities of vanadium–oxygen alloys with various compositions, $VO_{0.0834}$, $VO_{0.1127}$, $VO_{0.1245}$, and $VO_{0.1296}$, were measured from 320 to 920K by adiabatic scanning calorimetry. A heat capacity anomaly due to order–disorder rearrangement of oxygen atoms was observed for all the compositions. The transition temperatures from α′ to β phase were found to be 780, 791, 786, and 768K for $VO_{0.0839}$, $VO_{0.1127}$, $VO_{0.1245}$, and $VO_{0.1296}$, respectively. The transition temperatures from β′ to β were also observed to be 665 and 660K for $VO_{0.1245}$ and $VO_{0.1296}$, respectively, but they shifted to lower temperatures in repeated measurements. The excess heat capacity due to order–disorder transition was obtained by assuming that the heat capacity can be expressed as the sum of a harmonic term of lattice vibration, a dilational term, an electronic term, and an anharmonic term of lattice vibration. The entropy changes due to the transition for $VO_{0.0834}$, $VO_{0.1127}$, $VO_{0.1245}$, and $VO_{0.1296}$ were determined from the excess heat capacities to be 1.90, 2.88, 2.82, and 2.88 J K^{-1} $mole^{-1}$, respectively, values which were explained by calculating the entropy changes due to the order–disorder rearrangement of oxygen atoms in the superstructures of VO_x alloys. From the O/V dependence of the transition temperature and entropy change, the most stable composition of the α′ phase was thought to be $V_{48}O_5$.

1. Introduction

Interstitial atoms like oxygen, nitrogen, and carbon are known to distribute in octahedral sites in vanadium metal with body-centered cubic structure (*1, 2*) and form long-range ordered structures (*3–5*). Phase studies (*3, 6–8*) on the vanadium-rich oxygen alloy have shown that there are three phases, α, α′, and β′, at low temperatures for the O/V compositions, 0–0.04, 0.08–0.13, and 0.16–0.3, respectively. The structural study of these phases has been done by many investigators (*3, 9–11*). In the α phase, the oxygen atoms are distributed in octahedral sites (O_x, O_y, O_z) in a *bcc* metal subcell, where the O_x, O_y, and O_z sites have their neighboring metal atoms along the axes *x*, *y*, and *z*, respectively. In the α′ phase, the oxygen atoms preferentially occupy octahedral O_x and O_y sites to give tetragonal symmetry and form a superstructure with 4 × 4 × 6 metal subcells (*3, 10*). Similarly in the β′ phase, the oxygen atoms prefer to occupy the O_z site, giving tetragonal symmetry, and form a superstructure with 4 × 4 × 2 metal subcells (*11*). In the β phase, the high-temperature form of both α′ and β′ phases, oxygen atoms preferentially occupy octahedral O_z sites to give tetragonal symmetry without long-range ordering (*6, 12*). Order–disorder phase transitions from α′ to β and from β′ to β have been observed around 780 and 670K, respectively, using X-ray diffraction (*7, 8*) and heat capacity measurement (*3*).

In nonstoichiometric compounds such as VO_x, the change in heat capacity due to the

0022-4596/83/020162-10$03.00/0

compositional change is usually small, as the Kopp–Neumann law predicts, so long as the classical lattice vibration is predominant in the heat capacity (*13*). However, when phase transition occurs, as in the cases of TiO_x (*14*), $Ni_{1-x}Se_x$ (*15*), U_4O_{9-y} (*16*), $Mn_xFe_{3-x}O_4$ (*17*), and $Fe_{3-x}Cr_xO_4$ (*18*), the heat capacity and resulting enthalpy and entropy changes due to the transition vary with composition, which would give useful information for understanding the mechanism of the transition.

Hiraga and Hirabayashi (*3*) measured the heat capacity of VO_x with various O/V ratios and found that the entropy changes measured for the transition were much smaller than the calculated values based on the superstructure proposed by them.

In this paper, we measured the heat capacity of VO_x with x values 0.0834, 0.1127, 0.1245, and 0.1296, and the entropy change due to the phase transition was obtained as a function of composition by resolving the heat capacity into harmonic vibrational, dilational, anharmonic vibrational, electronic, and excess terms. The thermal expansion of $VO_{0.1127}$ has also been measured with the use of high-temperature X-ray diffraction, in order to estimate the dilational term of the heat capacity.

2. Experimental

2.1. Sample Preparation

V metal flake and V_2O_5 powder were used as received. The purity of the V metal was more than 99.7% and the major impurities were Mo (0.02%). As (0.005%), and Fe (0.005%). It was washed with dilute HCl solution and dried before use. The purity of the V_2O_5 powder was 99.99%, and it was reduced to V_2O_3 by heating it for 18 hr at 900°C in a hydrogen gas stream. The V metal flake and V_2O_3 powder were mixed in an appropriate ratio and melted a few times using a plasma jet furnace. The sample was sealed in a quartz tube, annealed two days at 1000°C, and cooled to room temperature over a period of 6 days. The sample was crushed into less than 3 mm in size using a stainless-steel mortar. The O/V ratio of the sample was determined from the weight gain of the sample by oxidizing it to V_2O_5 at 650°C for 3 weeks.

2.2. Heat Capacity Measurement

Heat capacities of VO_x were measured with an adiabatic scanning calorimeter (*19*); in this calorimeter the power supplied to the sample was measured continuously, and the heating rate was kept constant regardless of the kind and amount of sample. The heating rate chosen was 2K min^{-1}, and the measurement was carried out between 320 and 920K under a pressure of about 130 Pa of nitrogen. The heating rate and adiabatic control were usually maintained within ± 0.005K min^{-1} and ± 0.01K, respectively. The crushed sample was sealed in a quartz vessel filled with helium gas at about 20 kPa. The sample was annealed at 870K and cooled to room temperature over a period of 1 week before measurement.

2.3. High-Temperature X-Ray Diffraction

High-temperature X-ray diffractometry of $VO_{0.1127}$ was carried out in order to estimate the dilational term of the heat capacity of VO_x. Details of the technique were described elsewhere (*20*). X-Ray diffraction lines were observed in an argon gas atmosphere at about 1 kPa in the temperature range from room temperature to 810K. The scanning rate for 2θ was 0.25° min^{-1}, and the measurement was carried out in a short period to avoid oxidation of the sample.

3. Results

3.1. Heat Capacity of VO_x

The results of the heat capacity measurement on $VO_{0.0834}$, $VO_{0.1127}$, $VO_{0.1245}$, and

TABLE I

HEAT CAPACITY OF VO_x

T (K)	$VO_{0.0834}$ (MW, 52.276)	$VO_{0.1127}$ (MW, 52.745)	$VO_{0.1245}$ (MW, 52.933)	$VO_{0.1296}$ (MW, 53.015)
320	26.96	27.49	27.68	27.84
360	27.74	28.30	28.49	28.76
400	28.39	29.07	29.16	29.50
440	28.92	29.78	29.87	30.14
500	29.88	30.69	30.70	31.14
540	30.88	31.40	31.19	32.20
600	32.15	32.51	32.64	34.20
640	33.31	33.40	33.92	36.39
655	33.53	33.66	34.88	37.26
660	33.85	33.85	35.80	37.57
665	33.95	33.94	36.67	36.57
700	35.00	34.66	34.91	35.72
740	37.12	36.38	36.93	40.66
760	38.76	38.15	40.70	63.41
768	42.11	40.54	46.50	75.68
780	70.24	55.22	82.85	41.66
784	62.37	78.22	93.28	37.04
786	56.71	98.40	96.27	36.65
790	39.11	113.18	82.77	36.57
800	33.71	53.19	36.04	36.58
860	34.09	36.32	36.30	37.24
920	34.32	36.68	36.68	37.53

$VO_{0.1296}$ are listed in Table I and are also shown in Figs. 1 and 2. As seen in the figures, a heat capacity anomaly due to order–disorder transition from the α′ to β phase is observed around 780K for each sample and another anomaly from the β′ to β phase is observed around 660K for $VO_{0.1245}$ and $VO_{0.1296}$. The transition temperatures are listed in Table II. The measurement was carried out repeatedly for the same sample without annealing, and the results were essentially the same within the error of ±0.5% except for the vicinity of the peak of the heat capacity. The transition temperatures obtained in the second run are also listed in Table II. It is seen that the transition temperatures obtained in the second run are nearly the same as those in the first run for the transition from α′ to β, but for the transition from β′ to β they shift considerably to the lower-temperature side, and the shape of heat capacity anomaly changes, as shown by the dotted curve in Fig. 2. This would indicate the effect of

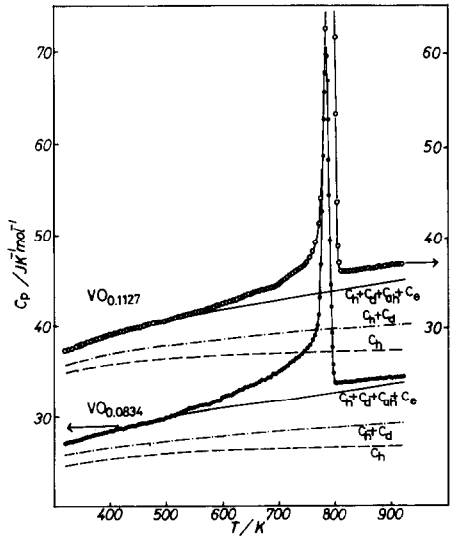

FIG. 1. Heat capacity of $VO_{0.0834}$ and $VO_{0.1127}$. The left-hand ordinate, the plots, and the resolution of heat capacity shown on the lower side are for $VO_{0.0834}$. The right-hand ordinate, the plots, and the resolution of heat capacity shown on the upper side are for $VO_{0.1127}$.

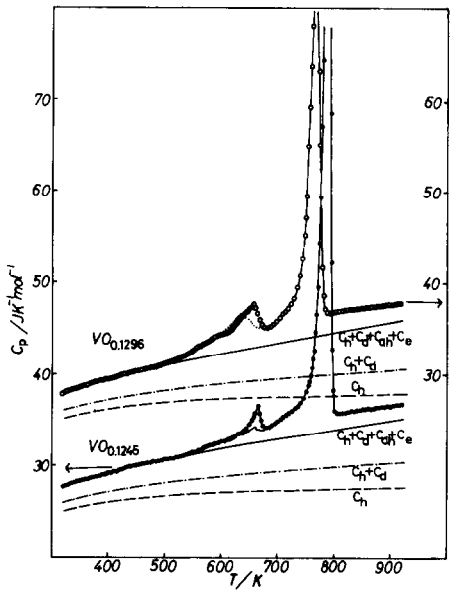

FIG. 2. Heat capacity of $VO_{0.1245}$ and $VO_{0.1296}$. The left-hand ordinate, the plots, and the resolution of heat capacity shown on the lower side are for $VO_{0.1245}$. The right-hand ordinate, the plots, and the resolution of heat capacity shown on the upper side are for $VO_{0.1296}$. The dotted lines shown between 600 and 700K are the data for the second run.

TABLE II

TRANSITION TEMPERATURES AND THE ENTROPY CHANGE FOR THE REACTION

O/V	Transition temperature T (K) First run	Second run	Entropy change ΔS (J K^{-1} mole^{-1})
0.0834	780(α′ to β)	779	1.90 ± 0.06[b]
0.1127	791(α′ to β)	791	2.88 ± 0.07[b]
0.1245	665(β′ to β) 786(α′ to β)	662 784	[a]2.82 ± 0.09[b]
0.1296	660(β′ to β) 768(α′ to β)	632 768	[a]2.88 ± 0.09[b]

[a] The sum of entropy change for the transitions α′ → β and β′ → β is given.
[b] The error due to measurement of heat capacity only is estimated.

quenching of the sample; the cooling rate of the sample in the calorimeter is too fast to be ordered completely from β to β′.

3.2. *Temperature Dependence of the Lattice Constant of $VO_{0.1127}$*

Figure 3 shows the temperature dependence of the lattice constant of $VO_{0.1127}$ obtained by high-temperature X-ray diffraction. The lattice constants obtained at room temperature, $a = 0.3112$ and $c = 0.2991$ nm, are in good agreement with those by Hiraga and Hirabayashi (*3*) and Henry *et al.* (*7*). Anomalies in the thermal expansion observed higher than 480K are thought to be due to an order–disorder transition from the α′ to β phase. Below about 480K, where a linear thermal expansion is observed, the temperature dependence of the lattice constant can be expressed as

$$a\ (\text{nm}) = 0.3111\{1 + 1.800 \times 10^{-5} \cdot (T - 273)/\text{K}\}, \quad (1)$$

$$c\ (\text{nm}) = 0.2990\{1 + 0.669 \times 10^{-5} \cdot (T - 273)/\text{K}\}, \quad (2)$$

where T indicates the temperature in degrees Kelvin.

4. Discussion

4.1. *Resolution of Heat Capacity*

The heat capacity of VO_x, C_p, is expressed by the sum

$$C_p = C_h + C_d + C_{ah} + C_e + \Delta C, \quad (3)$$

where C_h is the harmonic term of the lattice vibration, C_d the dilational term, C_{ah} the anharmonic term of the lattice vibration, C_e the electronic term, and ΔC the excess heat capacity due to order–disorder transition. Hence the excess heat capacity ΔC can be obtained by subtracting the terms C_h, C_d, C_{ah}, and C_e from the measured C_p.

4.1.1. Harmonic term of lattice vibration. The harmonic term of the lattice vibration is estimated from the data of elastic constants (*21*) and neutron inelastic scattering (*22*) as follows. Greiner *et al.* (*21*) measured the elastic constants of vanadium–oxygen alloy as a function of O/V ratio up to O/V = 0.0358, where the crystal structure is *bcc* α phase. Using Houston's method applied to

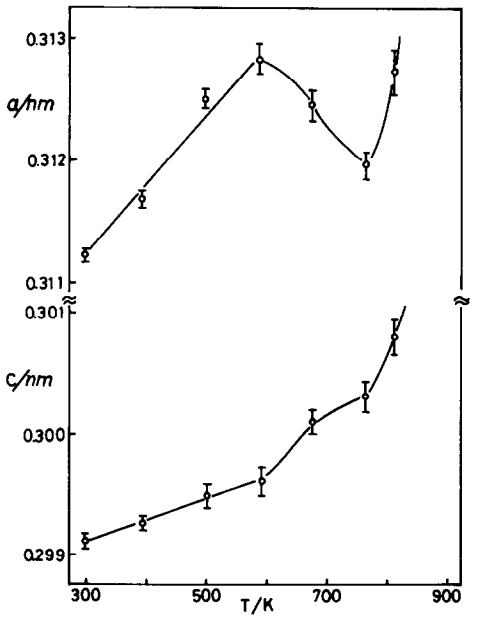

FIG. 3. Lattice constants of a and c axes of $VO_{0.1127}$ as a function of temperature.

cubic crystals (*23*), the Debye temperature can be expressed as

$$\Theta = \frac{h}{k}(9s/\Delta)^{1/3}J^{-1/3}, \qquad (4)$$

where Δ is the cell volume, s the number of atoms per cell, h Planck's constant, k Boltzmann's constant, and J is the constant determined by elastic constants C_{11}, C_{12}, and C_{44}. Using Eq. (4) and the values of C_{11}, C_{12}, and C_{44} at 300K (*21*), Debye temperatures for $VO_{0.0002}$, $VO_{0.0108}$, $VO_{0.0188}$, and $VO_{0.0358}$ are calculated to be 387.6, 395.6, 403.4, and 411.9K, respectively; these are plotted against O/V in Fig. 4. Sumin *et al.* (*22*) measured the neutron inelastic scattering spectrum at 300K for $VO_{0.031}$ and $VO_{0.205}$ samples. In the case of $VO_{0.031}$, the Debye model is suitable to represent the frequency spectrum as an approximation since the intensity of the optical branch was found to be negligibly small. The application of a Debye model to the case of $VO_{0.031}$ yields a Debye temperature of 409K. In the case of $VO_{0.205}$, the spectrum was similar to that of $V_{0.031}$ in the low-energy region and the cutoff energy 36.5 meV (424K) was determined by the Debye model, but two additional peaks were observed at 60 (696K) and 82 meV (952K). These are assigned to

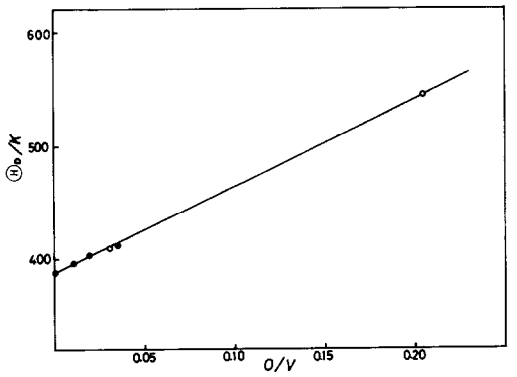

FIG. 4. Single Debye parameter as a function of O/V ratio. ●, calculated from elastic constants (*21*); ○, estimated from the data of neutron inelastic scattering (*22*).

optical modes coming from the local vibrations of oxygen atoms. Therefore, the harmonic heat capacity C_h for $VO_{0.205}$ can be expressed as

$$C_h = 3R\{D(424/T) + 0.205 \times \tfrac{2}{3}E(696/T) + 0.205 \times \tfrac{1}{3}E(952/T)\}, \qquad (5)$$

where $D(x)$ is the Debye function, $E(x)$ the Einstein function, and the factors $\frac{2}{3}$ and $\frac{1}{3}$ are determined by taking into account the degeneracy of the local modes, which are polarized along the faces perpendicular and parallel to the c axis, respectively. Since Eq. (5) is not expressed with a single parameter, the value of C_h expressed by Eq. (5) is fitted at 300K by a single Debye function,

$$C_h = (1 + x) \cdot 3R \cdot D(\theta_D/T), \qquad (6)$$

where x is O/V ratio.

For $x = 0.205$ we obtain the Debye temperature $\theta_D = 545$K. These Debye temperatures thus determined for $VO_{0.031}$ and $VO_{0.205}$ are also shown in Fig. 6, where a fairly good linear relationship between O/V and Debye temperature is observed. Small deviations from the linear line for $VO_{0.031}$ and $VO_{0.0358}$ are thought to be due to disregard of optical modes, which increase as O/V increases. A similar linear relationship has also been observed in the systems such as NbO_x (*24*), VC_x (*25*), and NiH_x (*26*). The increase of the Debye temperature with O/V ratio corresponds to similar behavior of hardness with O/V (*6*). By interpolation of the linear relationship shown in Fig. 4, the Debye temperatures for $VO_{0.0834}$, $VO_{0.1127}$, $VO_{0.1245}$, and $VO_{0.1296}$ are determined to be 453, 477, 486, and 490K, respectively, and then the harmonic term of the lattice vibration C_h is calculated as shown in the broken lines in Figs. 1 and 2.

4.1.2. Dilational term. The dilational term of the heat capacity C_d can be expressed as

$$C_d = \Gamma\beta C_v T, \qquad (7)$$

$$\Gamma = V\beta/(\kappa C_v), \tag{8}$$

where Γ is the Grüneisen parameter, which is nearly constant with temperature variation, β the thermal expansivity, C_v the heat capacity at constant volume, V the molar volume, and κ the isothermal compressibility. The value of Γ for $VO_{0.1127}$ is estimated as follows: the compressibility κ is calculated from the elastic constants using the relation for a cubic crystal,

$$1/\kappa = \tfrac{1}{3}(C_{11} + 2C_{12}), \tag{9}$$

where $1/\kappa$ is the isothermal bulk modulus. The value of $1/\kappa$ at 300K is obtained as a function of O/V up to O/V = 0.0358 using the data by Greiner *et al.* (*21*), and it is extrapolated to $VO_{0.1127}$, from which the value of κ for $VO_{0.1127}$ is obtained to be 6.235×10^{-12} Pa^{-1}. The molar volume V is calculated from lattice constants a and c at room temperature and the expansivity β is obtained from Eqs. (1) and (2). Then, Γ for $VO_{0.1127}$ is determined as 2.24. The values of Γ for other compositions are assumed to be the same as 2.24 and the dilational terms C_d for all the compositions are calculated by Eq. (7). The calculated values $C_h + C_d$ are shown in Figs. 1 and 2.

4.1.3. Electronic and anharmonic terms of the heat capacity. We have no available data to estimate the electronic and anharmonic terms of the heat capacity as a function of O/V ratio. Accordingly, it is assumed that at lower temperatures the excess heat capacity is negligibly small and the sum of the electronic and anharmonic terms can be calculated from the experimental data as the following,

$$C_p - C_h - C_d = C_e + C_{ah} = (\gamma + b)T, \tag{10}$$

where γ is the coefficient of the high-temperature electronic heat capacity and b is the coefficient of anharmonic heat capacity. Using the observed values of C_p between 320 and 450K and the calculated values of

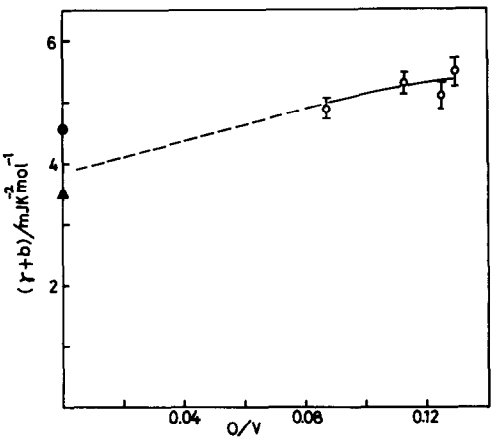

FIG. 5. Sum of the coefficients of electronic and anharmonic heat capacities as a function of O/V ratio at high temperatures. ○, The present study; the range marked at the plot shows the estimated error. ●, The datum estimated by Shimizu *et al.* (*27*) using heat capacity data at high temperatures. ▲, The datum obtained from heat capacity measurement at high temperatures (*29*).

C_h and C_d, the value of $(\gamma + b)$ is determined with the condition that the term $(C_p - C_h - C_d)$ vanishes at 0 K. The sums thus determined, $C_h + C_d + C_e + C_{ah}$, for various O/V ratios are shown in Figs. 1 and 2. The value of $(\gamma + b)$ obtained is shown in Fig. 5 as a function of O/V ratio. It is seen from Fig. 5 that $(\gamma + b)$ increases gradually with O/V ratio. Shimizu *et al.* (*27*) have reported the values of the coefficient of electronic heat capacity γ for pure vanadium as a function of temperature from both a theoretical calculation and an estimation using data of high-temperature heat capacity (*28*). They have found that γ has a high value of 8.9 mJ K^{-2} mole^{-1} at 0 K and decreases with increase of temperature, and about 4.6 mJ K^{-2} mole^{-1} in the range between 300 and 900K. Kohlhaas *et al.* (*29*) have reported the γ value at high temperatures to be around 3.5 mJ K^{-2} mole^{-1} from the measurement of high-temperature heat capacity. A similar value for $(\gamma + b)$ of vanadium metal at high temperatures has also been obtained recently by Takahashi (*30*)

using laser flash calorimetry. The (γ + b) value extrapolated to O/V = 0 in Fig. 5 seems to be in good agreement with these values for pure vanadium metal. In the cases of NbO_x (*24*), TiO_x (*31*), and VH_x (*32*), γ decreases as the oxygen-to-metal ratio increases, since oxygen atoms may be negatively charged. If it is true in VO_x, the increase of the coefficient of anharmonic heat capacity b with O/V should be larger than the decrease of γ with O/V, since (γ + b) increases with O/V as shown in Fig. 5. The increase of the anharmonic term with O/V may be caused by destruction of the local symmetry of the lattice by the introduction of interstitial oxygen atoms.

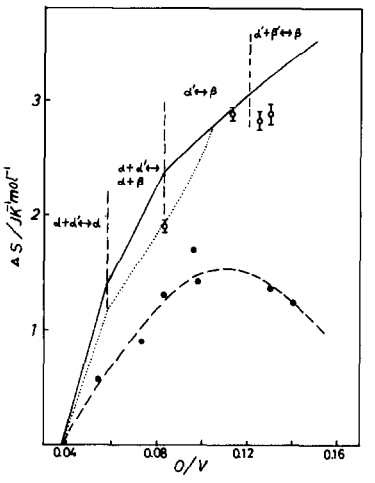

FIG. 6. Observed and calculated entropy changes for the order–disorder transition. O, Observed data; the range marked at the plot shows the experimental error. ●, Data by Hiraga and Hirabayashi (*3*). ——, Calculated values according to Eqs. (11)–(13). ····, Calculated values according to Eq. (14) as well as Eqs. (11)–(13).

4.2. Entropy Change due to Order–Disorder Transition

The excess heat capacity ΔC calculated from Eq. (3) is shown in Figs. 1 and 2 as a function of temperature, where the values of the terms C_h, C_d, C_e, and C_{ah} are estimated as described in the preceding section. At 920K, the highest temperature in this experiment, it is seen that ΔC still has a finite value, showing the presence of short-range ordering at higher temperatures. The short-range ordering in the order–disorder transitions is a well-known feature in alloy systems (*33, 34*), and Kirkwood's theory (*35*) predicts that the excess heat capacity ΔC changes with T^{-2} at far above transition temperatures. Hence the values of ΔC above 920K are estimated by extrapolation to a very high temperature assuming Kirkwood's theory. Thus the entropy change due to order–disorder transition can be obtained and the results are shown in Table II and Fig. 6, where the sum of the entropy changes for $\alpha' \rightarrow \beta$ and $\beta' \rightarrow \beta$ is shown for the samples with O/V larger than 0.12 and the error due to the measurement of heat capacity is shown for all the samples. The error due to estimation in the baseline heat capacity and due to extrapolation of the excess heat capacity to a high temperature are estimated to be the same order of magnitude as the experimental error. The results by Hiraga and Hirabayashi (*3*) are also shown in Fig. 6 for comparison. It is seen from Fig. 6 that the values by Hiraga and Hirabayashi (*3*) are considerably lower than ours in spite of small differences in heat capacity data between the two measurements. Their smaller entropy changes may be mainly due to overestimation of the baselines of the heat capacity data, although the method to determine the baseline was not described in their paper (*3*).

On the other hand, the entropy change due to the order–disorder transition is calculated theoretically as follows. In the $0.038 \leqq O/V \leqq 0.058$ region, the transition $\alpha + \alpha' \rightarrow \alpha$ occurs. Since oxygen atoms occupy any of the three octahedral sites O_x, O_y, and O_z in the α phase, the number of available oxygen sites is $3N$ (when the number of metal atoms is taken as N) and the entropy change ΔS_1 is calculated as follows, assuming the ordering in the α' phase

is perfect,

$$\Delta S_1 = a\,k \ln \frac{(3N)\,!}{(xN)\,!\,(3N - xN)\,!} = -aR\left\{(3 - x) \ln \frac{3 - x}{3} + x \ln \frac{x}{3}\right\}. \quad (11)$$

where a is the mole fraction of α' phase at low temperature, determined by the O/V ratio of sample, and x is the O/V composition of the α' phase ($x = 0.0833$). ΔS_1 is shown in a solid line in Fig. 6. In the O/V $\geqq$ 0.0833 region, the transition $\alpha' \rightarrow \beta$ occurs. Since oxygen atoms occupy only O_z sites in the β phase, the number of available oxygen sites is N and the entropy change ΔS_2 is

$$\Delta S_2 = k \ln \frac{N\,!}{xN\,!\,(N - xN)\,!} = -R\{x \ln x + (1 - x) \ln (1 - x)\}, \quad (12)$$

where $x \geqq 0.0833$, and perfect ordering in α' phase is assumed. ΔS_2 is shown as a solid line in Fig. 6. As will be shown later, the region of existence of the pure α' phase ends around O/V = 0.12 and the presence of a mixture of α' and β' phases is observed above O/V = 0.12. Hence Eq. (12) holds at compositions up to about O/V = 0.12. In the $0.058 \leqq$ O/V $\leqq 0.0833$ region, the transition $\alpha + \alpha' \rightarrow \alpha + \beta$ occurs and the entropy change ΔS_3 can be expressed by

$$\Delta S_3 = -0.44a'R\left\{(3 - x) \ln \frac{3 - x}{3} + x \ln \frac{x}{3}\right\} - (1 - a')R\{x \ln x + (1 - x) \ln (1 - x)\}, \quad (13)$$

where a' is the mole fraction of $\alpha' \rightarrow \alpha$, and $1 - a'$ is that of $\alpha' \rightarrow \beta$. ΔS_3 is also shown as a solid line in Fig. 6. As seen in Fig. 6, the calculated value of ΔS for $VO_{0.1127}$ is in good agreement with the observed one, but the observed values for other compositions are about 0.3 ~ 0.5 J K^{-1} $mole^{-1}$ smaller than the calculated ones. The discrepancy

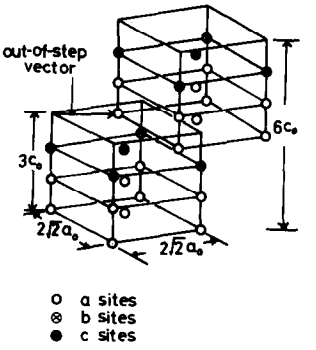

FIG. 7. The superstructure of α' phase ($4 \times 4 \times 6$ metal subcells) oxygen sites only are shown: sites a are the sites for $V_{12}O$, sites b are extra sites for $V_{48}O_5$, and sites c are extra sites for V_8O.

for $VO_{0.0834}$ may be explained by assuming the presence of the most stable α' phase $V_{48}O_5$ and partial disordering of the oxygen atoms for compositions below $VO_{0.104}$ in the α' phase. Hiraga and Hirabayashi (*3*) proposed a superstructure model of the α' phase as shown in Fig. 7, where the oxygen atoms in a sites are for $V_{12}O$ ($VO_{0.0833}$) and the additional oxygen atoms in b and c sites are for V_8O ($VO_{0.125}$). It has been found that the maximum transition temperature from α' to β is near the composition $VO_{0.1}$ by the present study and also by Hiraga and Hirabayashi (*3*), which may indicate that the structure of the α' phase is the most stable at this composition. If we take away oxygen atoms from the c sites shown in Fig. 7 for the V_8O structure, we obtain the $V_{48}O_5$ structure, which is thought to be the most stable one in the α' phase, as this composition is $VO_{0.104}$. When the O/V composition is less than $VO_{0.104}$, it can be assumed at low temperatures that there is a residual entropy due to the random removal of the oxygen atoms from a and b sites of the $V_{48}O_5$ structure. The residual entropy ΔS_4 at low temperature is then given as

$$\Delta S_4 = k \ln \frac{\left(\frac{5}{48}N\right)\,!}{\left(\frac{5}{48}N - \delta N\right)\,!\,(\delta N)\,!}$$

$$= -R\left\{\left(\frac{5}{48}-\delta\right)\ln\left(1-\frac{48}{5}\delta\right) + \delta\ln\frac{48}{5}\delta\right\}, \quad (14)$$

where O/V = 5/48 − δ and $0 \leqq \delta \leqq 1/48$ (δ = 1/48 corresponds to the composition limit of the pure α′ phase, $V_{12}O$). The resulting entropy change from α′ to β is expressed by $(\Delta S_2 - \Delta S_4)$ and is shown as a dotted line in Fig. 6, where it is seen that the observed entropy change ΔS for $VO_{0.0834}$ is close to this line.

In the case of higher O/V compositions, $VO_{0.1245}$ and $VO_{0.1296}$, a heat capacity anomaly due to the β′ → β transition is observed besides that due to α′ → β transition, which indicates that the sample is a mixture of α′ and β′ phases at low temperature for these O/V compositions. It is noted that the observed entropy changes obtained by Hiraga and Hirabayashi (*3, 11*) for the β′ → β transition at O/V compositions higher than 0.16 are much smaller than the calculated ones according to Eq. (12), even though their possible overestimation of the baseline heat capacity is taken into account, which shows the existence of partial disordering of oxygen atoms in the β′ phase. The smaller than calculated values observed for the entropy change of $VO_{0.1245}$ and $VO_{0.1296}$ may be understood as being due to the partial disordering of oxygen atoms in the β′ phase.

Acknowledgment

The authors wish to thank Mr. M. Iseki for his aid in making samples by use of a plasma jet furnace.

References

1. K. Hiraga, T. Onozuka, and M. Hirabayashi, *Mater. Sci. Eng.* **27,** 35 (1977).
2. J. Takahashi, M. Koiwa, M. Hirabayashi, S. Yamaguchi, Y. Fujino, K. Ozawa, and K. Doi, *J. Phys. Soc. Japan* **45,** 1690 (1978).
3. K. Hiraga and M. Hirabayashi, *Trans. JIM* **16,** 431 (1975).
4. D. Potter and C. Altstetter, *Acta Metall.* **19,** 881 (1971).
5. K. Hiraga and M. Hirabayashi, *J. Appl. Crystallogr.* **13,** 7 (1980).
6. A. U. Seybolt and H. T. Sumsion, *Trans. AIME* **197,** 292 (1953).
7. J. L. Henry, S. A. O'Hare, R. A. McCune, and M. P. Krug, *J. Less-Common Met.* **21,** 115 (1970).
8. D. G. Alexander and O. N. Carlson, *Metall. Trans.* **2,** 2805 (1971).
9. K. Hiraga, H. Ikeda, and M. Hirabayashi, *Japan. J. Appl. Phys.* **19,** 397 (1980).
10. D. Gunwaldsen and D. Potter, *J. Less-Common Met.* **34,** 97 (1974).
11. K. Hiraga and M. Hirabayashi, *J. Phys. Soc. Japan* **34,** 965 (1973).
12. C. W. Tucker, A. U. Seybolt, and H. T. Sumsion, *Acta Metall.* **1,** 390 (1953).
13. H. Inaba and K. Naito, *Netsusokutei* **4,** 10 (1977).
14. M. Koiwa and H. Hirabayashi, *J. Phys. Soc. Japan* **27,** 801 (1969).
15. F. Grønvold, N. J. Kveseth, and A. Sveen, *J. Chem. Thermodyn.* **7,** 617 (1975).
16. H. Inaba and K. Naito, *J. Nucl. Mater.* **49,** 181 (1973).
17. K. Naito, H. Inaba, and H. Yagi, *J. Solid State Chem.* **36,** 28 (1981).
18. H. Inaba, S. Nakashima, and K. Naito, *J. Solid State Chem.* **41,** 213 (1982).
19. K. Naito, H. Inaba, M. Ishida, Y. Saito, and H. Arima, *J. Phys. E* **7,** 464 (1974).
20. K. Naito, T. Tsuji, and T. Matsui, *J. Nucl. Mater.* **48,** 58 (1973).
21. J. D. Greiner, O. N. Carlson, and J. F. Smith, *J. Appl. Phys.* **50,** 4394 (1979).
22. V. V. Sumin, S. A. Danilkin, and S. I. Morozov, *Sov. Phys. Solid State* **20,** 1001 (1978).
23. D. D. Betts, A. B. Bhatia, and M. Wyman, *Phys. Rev.* **104,** 37 (1956).
24. C. C. Koch, J. O. Scarbrough, and D. M. Kroeger, *Phys. Rev. B* **9,** 888 (1974).
25. V. S. Chernyaev, E. N. Tzetnikov, G. N. Shveikin, R. N. Krentzis, and P. V. Gelitz, *Izv. Acad. Nauk SSSR Neorg. Mater.* **3,** 789 (1967).
26. G. Barkleit and G. Wolf, *Phys. Status Solidi A* **28,** 139 (1975).
27. M. Shimizu, T. Takahashi, and A. Katsuki, *J. Phys. Soc. Japan* **18,** 1192 (1963).

28. "American Institute of Physics Handbook," Vol. 4, p. 40, McGraw–Hill, New York (1957).
29. R. KOHLHAAS, M. BRAUN, AND O. VOLLMER, *Z. Naturforsch. A* **20,** 1077 (1965).
30. Y. TAKAHASHI, private communication.
31. M. HIRABAYASHI, S. YAMAGUCHI, H. ASANO, AND K. HIRAGA, "Order–Disorder Transformations in Alloys" (H. Warlimont, Ed.), p. 266, Springer-Verlag, New York/Berlin (1974).
32. D. OHLENDORF AND E. WICKE, *J. Phys. Chem. Solids* **40,** 721 (1979).
33. C. SYKES AND F. W. JONES, *Proc. Roy. Soc. Ser. A* **157,** 213 (1936).
34. J. M. COWLEY, *Advan. High Temp. Chem.* **3,** 35 (1971).
35. J. G. KIRKWOOD, *J. Chem. Phys.* **6,** 70 (1938).